A simple method for the quantification of molecular decorations on silica particles

Daniel N Mangos[1,2]**, Takashi Nakanishi**[2] **and David A Lewis**[1]

[1] Centre for NanoScale Science and Technology, Flinders University of South Australia, GPO Box 2100, Adelaide 5001 Australia
[2] National Institute for Materials Science (NIMS), Tsukuba 305-0047, Japan

E-mail: david.lewis@flinders.edu.au

Abstract

A simple, rapid quantitative approach to determining attachment density on silica nanoparticles has been demonstrated using attenuated total reflectance Fourier transform infrared spectroscopy and verified by thermogravimetric analysis. A very high attachment of approximately 5 attachments per nm^2 has been achieved through photoinduced thiol–ene click reaction of 11-bromo-1-undecene with a thiol functionalized silica nanoparticle formed from mercaptopropyltrimethoxysilane as the sole precursor. Attachment density with concentration of alkene and reaction time is shown to be highly nonlinear and appears to be limited by accessability of thiols on the surface of the particle. This method opens the opportunity to form nanoparticles with controlled functionality including multifunctional particles, which have been produced in this work.

Keywords: sol–gel, thiol–ene click chemistry, ATR-FTIR, quantitative functionalization, silica nanoparticles

S Online supplementary data available from stacks.iop.org/STAM/15/015002/mmedia

1. Introduction

Silica nanoparticles (SiNPs) are attractive candidates for use as a platform material to deliver functionality to a wide range of applications including cosmetic products, biosensors and to enhance the mechanical properties of coatings and composite materials [1–5]. The key attribute is that they are chemically and biologically inert and the size can be tuned for a specific application. While the particle can be both a carrier and the functional component, the surface of the particle is ultimately responsible for delivering the specific functionality as it controls dispersion, how the particle interacts with the surroundings as well as potentially carrying targeting moieties. The ability to controllably modify the surface of substrates has led to the improved performance and versatility of various functional materials, and to do this in a controllable manner is naturally desirable [6–9].

Particle dispersion and surface modification can be achieved by the physical adsorption of small or large molecules. The physically adsorbed polymer can be subsequently modified, however, the modifiers can have a fugitive effect due to weaker surface interactions, and the original SiNP surface can be regenerated, which can cause the particles to aggregate [10].

Permanent surface modification can be achieved through the activation and subsequent reaction of hydroxyl groups on the surface of the silica particle. Other functionalities can be delivered through the use of functional trimethoxysilanes such as gamma epoxy trimethoxy silane, vinyl trimethoxysilane and gamma mercapto trimethoxy silane (MPTMS), but these tend to be limited by the need for tetraorthosilicate (TEOS) to form spherical particles that are uniform in size, resulting in comparatively low functional density. MPTMS, however, has been demonstrated to produce spherical particles as a sole alkyl-silane precursor to create highly functional particles [11], removing the need for TEOS as a filling agent.

The high density of thiol groups on the particle surface provided by condensed MPTMS is an ideal platform to

attachment a wide range of molecules through thiol–ene click chemistry. In solution, thiol–ene chemistry is a high yielding process that is relatively easy to initiate over a wide range of temperatures and conditions [12] and has been used for the end group modification of block polymers to generate macromolecules with complex architectures [13]. The capability of thiol moieties to scavenge free radicals assists their regeneration after successful attachment of a thiol–ene bond, effectively acting as a chain transfer process [14] which has potential as a relatively benign means to functionalize particles. However, free radical thiol–ene approaches to form polymeric particle structures and control ligand orientation on magnetic nanoparticles have only been reported to achieve attachment densities of about 0.55 alkene attachments per nm^2 using phosphonic acid derivatives [15], which is significantly lower than other high density attachment mechanisms that currently yield 2–5 attachments per nm^2, which utilize cycloaddition and ring opening chemical processes [16, 17].

The application of thiolated particles is becoming increasingly relevant as functionalization of the thiol-moeity lends itself to applications including bioimaging and molecular recognition [18], requiring the number and type of adduct to be controlled. It has been established that thiol terminated surfaces can be utilized to generate fluorescent markers for bio-imaging through the attachment of rhodamine red maleimide [11], however the control and quantification of the functionalization density of such systems is yet to be demonstrated, and of increasing importance. Simple and reliable methods are necessary to quantify the level of functionalization and subsequently controlling the attachment density is necessary to establish future platform capabilities and advance this field.

In this work, the use of attenuated total reflection Fourier transform infrared spectroscopy (ATR-FTIR) is used to quantify the attachment density through the use of a simple calibration approach using internal standards. This technique is then used to quantify the attachment density of alkenes to SiNPs of controlled size using photoinitiated thiol–ene click reaction at ambient temperature.

2. Experimental details

2.1. Chemicals and reagents

3-Mercaptopropyltrimethoxysilane (MPTMS) (95%), benzophenone ($>99\%$), 11-bromo-1-undecene (95%) and 10-bromo-1-undecene (95%) were purchased from Sigma-Aldrich and used as received. Azobisisobutyronitrile (AIBN) and ethanol (absolute) were purchased from Merck.

2.2. Synthesis and functionalization conditions of SiNP's

A stable colloidal suspension of thiol functionalized SiNPs was prepared by dropwise addition of MPTMS (57 μl, 3.07×10^{-4} mol) for d_{avg} 170 nm to a blend of 28% ammonia (3.60 ml) and deionized water (46.4 ml) and allowed to stir at room temperature for 3 days at 550 rpm [11].

For nanoparticle functionalization in the photo generated free radical systems, 11-bromo-1-undecene (0.15 ml, 6.8×10^{-4} mol) and benzophenone photo initiator (23.3 mg, 1.3×10^{-4} mol) were added to 25 ml of thiol terminated SiNPs solution. The mixture was stirred for 30 min under an Oriel Illuminator UV lamp Model 82420.

2.3. Analysis

Nanoparticle solutions were analysed using dynamic light scattering (DLS) with a Malvern Instruments 'High Performance Particle Sizer' model HPP5001. DLS measures the Brownian motion of a particle in a given solute, and parameters were set given the relative viscosity of the solvent and an approximation of the chemical composition of the particle. Correlation data was analysed using Malvern Instruments software.

The DLS measurements were made at the following specifications. Temperature, 25 °C; path length, 1 cm; attenuation index, 8; mean position, 1.6 mm; run duration, 12 scans. All runs were done in triplicate in monomodal mode.

Thermogravimetric analysis (TGA) was performed on the TA Instruments—Hi-res TGA 2950 using a temperature ramp of 10 °C min^{-1}. Thermal decomposition was recorded under 50 ml min^{-1} of N_2 gas.

Nanoparticles were prepared for scanning electron microscopy (SEM) imaging by coating with metal using a Quorumtech K575X sputter coater. A 10 nm platinum or gold coating was applied to the sample as measured using a film thickness monitor. Thiol functionalized particles were analysed using FEI Phenom^{TM} SEM.

FTIR measurements were performed on a Nicolet Nexus 870 FT-IR, equipped with a Thermo Scientific ATR-IR 'Smart Orbit Attachment'. The spectral data was collected at 4 cm^{-1} resolution with 64 scans at room temperature.

Surface area was determined experimentally by Brunauer–Emmet–Teller (BET) isotherm measurements on a micromeritics TriStar II 3030 surface area and porosity analyser. SiNPs were dried at 30 mbar and 60 °C overnight and then at 0.1 mbar at 90 °C for 3 h prior to isothermal analysis.

Kinetic control using photo irradiation was done under similar conditions to nanoparticle functionalization described earlier. The reaction was allowed to proceed for 1, 5, 10, 15 and 30 min respectively under the conditions specified in section 2.2.

For evaluation of supernatant liquid pre- and post-functionalization under photo irradiation conditions, samples were prepared for gas chromatography–mass spectrometry (GC–MS) using a Varian CP-3800 Gas Chromatograph attached to a Varian Saturn 2200 Mass Spectrometer by using the following methodology. Injector: 1:50 split ratio, 200 °C, flow rate: 1.2 ml min^{-1} of N_2 as the carrier gas, oven temperature starting at 80 °C and ramping to 280 °C at 20 °C min^{-1} and held for 10 min. 50 ml of sample was injected into a GC sample vial, and then made up to 1.38 ml using chloroform as the solvent.

For creation of the calibration curve 0.1, 0.2, 0.3, 0.4, 0.7, 0.9 and 1 μl of 11-bromo-1-undecene were added to 13 mg samples of thiol terminated SiNPs (with an average diameter
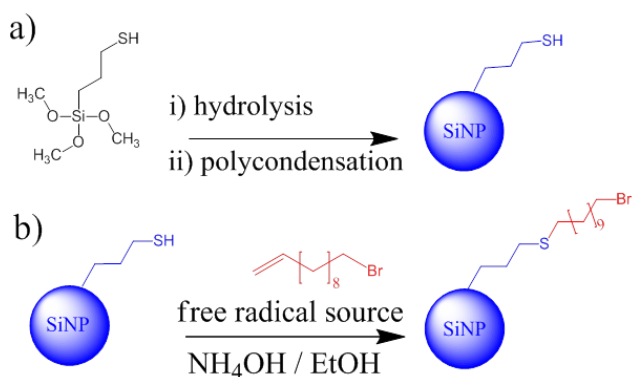
Scheme 1. (a) Formation of thiol terminated SiNP from MPTMS. (b) Thiol–ene click reaction occurring on the thiol terminated SiNP surface to produce bromoalkyl terminated SiNPs.

of 170 nm) via a GC syringe. Samples were homogenized with mortar and pestle, left to dry in vacuum overnight at 50 °C and analysed via ATR-FTIR spectroscopy. Calculations and examples of typical experimental data can be seen in the supporting information (available at stacks.iop.org/STAM/15/015002/mmedia).

3. Results and discussion

A sequential approach to the production of functionalized SiNPs has been used in this study, as shown in scheme 1. In the first step, thiol functionalized SiNPs are produced using a revised Stöber process [11]. In this process, a stable colloidal solution of particles is formed through hydrolysis and polycondensation of MPTMS in basic aqueous conditions using ammonia to form uniform spherical particles with a relatively narrow size distribution. In a subsequent step, a free radical source (photo, thermal or chemical initiator) and the desired alkene are added directly to the colloidal solution in a simple one pot two step system.

Particle size can be controlled by the precursor concentration and taking the reaction to completion as demonstrated by Nakamura and Ishimura [11], who showed the particle diameter could be controllably varied between 220 and 700 nm. Particles with an average diameter of 25 and 170 nm were produced by using precursors at concentrations of 1.25 and 6.25 mM respectively, which extends the relationship between precursor concentration and particle size below 200 nm, as shown in figure 1. The particles were confirmed to be spherical and relatively uniform in size determined in both DLS and SEM, as shown in figure 2. In a modification of the Nakamura and Ishimura process, ethanol based solutions were observed to maintain their fidelity for the 72 h reaction time creating a colloidal stable system, while water-based systems agglomerated after 36 h. This was especially evident when larger reaction volumes were used.

The surface area of the 170 nm particles was determined to be 21.7 $m^2\,g^{-1}$ by BET which compares to a calculated value of 18.0 $m^2\,g^{-1}$ assuming a density of 2.0 $g\,cm^{-3}$ [19, 20]. The isotherm showed the sample was mesoporous with a porosity of about 30–45 nm, which is consistent with an agglomerate of solid 170 nm particles. All values use the experimentally determined value for surface area.
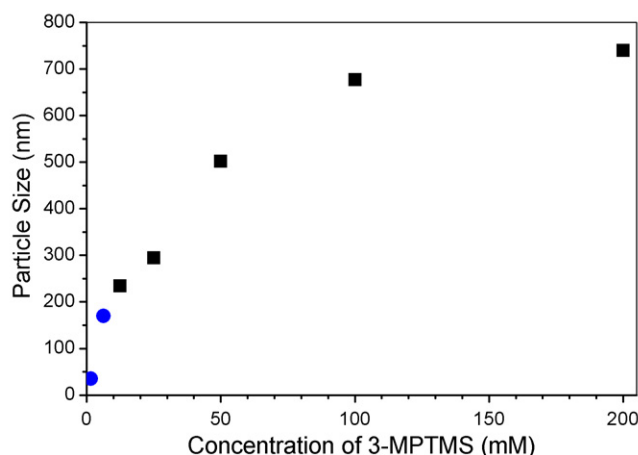

Figure 1. Extension of the relationship between silane precursor concentration and particle size (circles) and the size taken from Nakamura and Ishimura's result (squares).
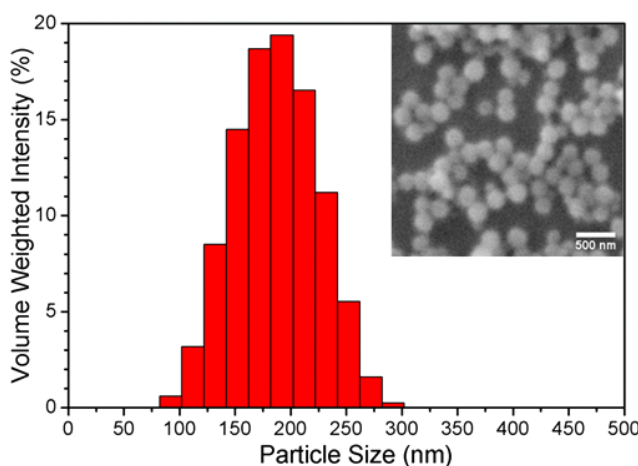

Figure 2. DLS measurement of SiNP hydrodynamic diameter. Inset shows SEM image of SiNPs.

ATR-FTIR analysis is a particularly attractive method to study nano-powders due to its non-destructive nature [21]. Quantitative ATR-FTIR analysis can be inherently difficult due to the need for a strong and reproducible 'level of contact' between the sample and the reflectance crystal [22], however, such reproducibility issues can be overcame by using a reliable IR active mode as an internal standard [23, 24]. Particle sizes in the nanoregime are known to not attenuate absorbance in the infrared region, however it has been established previously that as particle size enters the micron range, the detected absorbance can be significantly attenuated [22].

The oligo-methylene asymmetric stretching mode ν_{asym} (CH$_2$) at 2926 cm^{-1} (labelled **A** in figure 3) and the ν_{sym} (Si–O–Si) symmetrical bending peak at 1070 cm^{-1} (labelled **B**) are clearly resolved when 11-bromo-1-undecene is added directly to SiNP powder ($d_{avg} = 170$ nm) as can be seen in figure 3. Since the Si–O–Si bond is not directly involved in the modification process, it becomes an ideal reference band and the ratio of the ν_{asym} (CH$_2$) band can be seen to increase with respect to the normalized ν_{sym} (Si–O–Si) band in figure 4 with increasing alkene present.
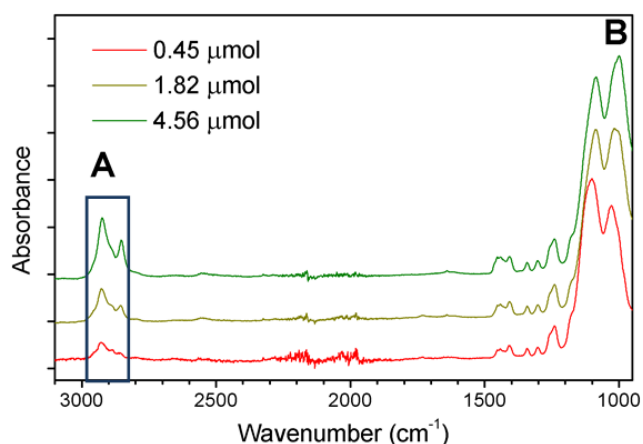
Figure 3. ATR-FTIR overlay of CH_2 stretching (labelled 'A') with various additions of 11-bromo-1-undecene, homogenized in SiNP powder. (Normalized to a common peak height for the Si–O–Si absorption labelled as 'B'.)
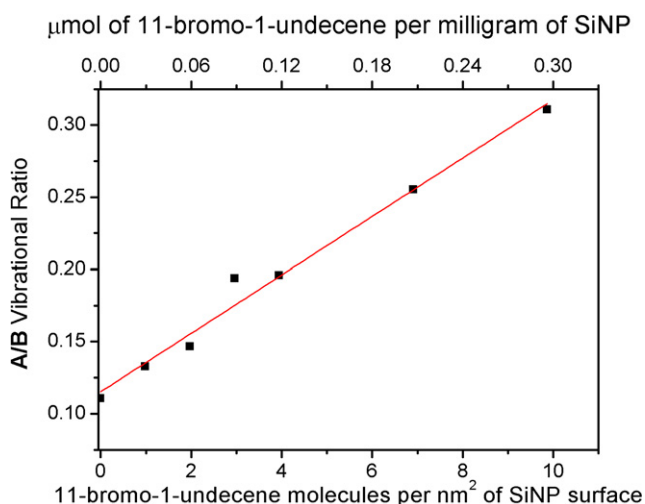

Figure 4. Calibration curve of addition of unattached alkene relative to surface area available, with a line of best fit, where error associated with measurement of A/B is ± 0.05.

Figure 5. Rate of surface attachment for 1.75 mmol of 11-bromo-1-undecene under UV irradiation.

Figure 6. TGA of unfunctionalized SiNPs (blue) and 10-bromodecane functionalized SiNPs (red) prepared from a 1.75 mmol concentration of 10-bromo-1-decene.

A calibration curve relating controlled amounts of alkene added to dried SiNP results in a linear relatonship as shown in figure 4. The resulting positive *x*-intercept is due to the methyl groups in the MPTMS precursor. Since the ratio of methylene to Si–O–Si is constant in mercaptopropyl trimethoxy silane based SiNP's, this intercept is constant and independent of particle size and the amount of SiNP on the ATR window. Given that the oligo-methylene (CH_2) vibrational band increases linearly with respect to concentration, this method can be used to track hydrocarbon functionalized attachment agents, provided that the detection threshold is within the linear range of the Beer–Lambert conditions.

Figure 5 shows the increase in attachment of 11-bromo-1-undecene with irradiation time, showing maximum functionalization density, corresponding to 4.9 attachments per nm^2, was achieved after 60 min of photoirradiation. No increase in the attachment density was observed with further photoirradiation, suggesting that accessible thiols were most-likely fully reacted, meaning surface thiols were fully reacted or any unreacted thiols
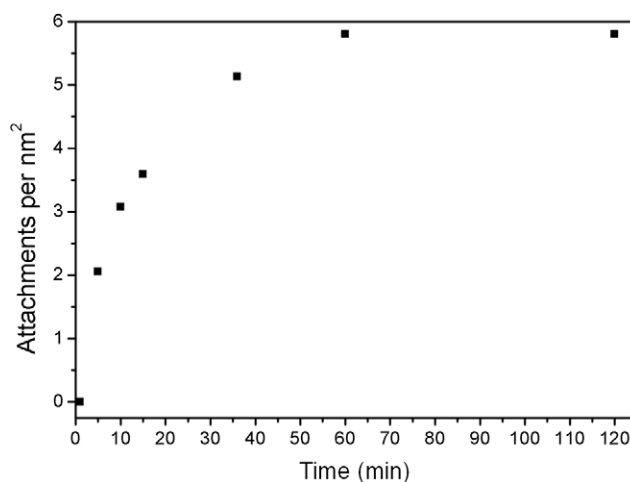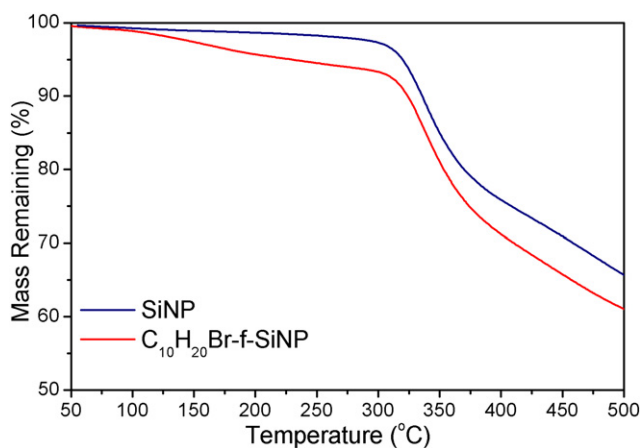
are no longer accessible. The example shown in figure 5 is for 1.75 mmol of unreacted alkene corresponding to 4450 alkene molecules in solution per nm^2 of particle surface or an approximate 800-fold excess of alkene to maximum surface attachments. At maximum attachment density, $0.15\,\mu mol$ of alkene attached per mg at complete density, corresponding to 4.9 attachments per nm^2 of SiNP surface, well within the calibration range of figure 4.

TGA has been used as an independent method to measure the attachment density and verify the FTIR analysis method. While the SiNP is stable to over $300\,°C$, the adduct loses mass from $100\,°C$ to about $250\,°C$, before following the weight-loss profile of the SiNP as shown in figure 6. This mass loss in the 100–$250\,°C$ range for the functionalized particle is believed to be due to the loss of the covalently attached alkene, with the weight loss profile and similarities in decomposition of comparable organic species [25]. The difference between the weight loss of the functionalized and non-functionalized SiNP is 4.4% at $290\,°C$. A mass loss difference of 4.4% for a 170 nm particle at maximum attachment density corresponds to 5.8 attachments per nm^2, which is similar to the attachment density determined by
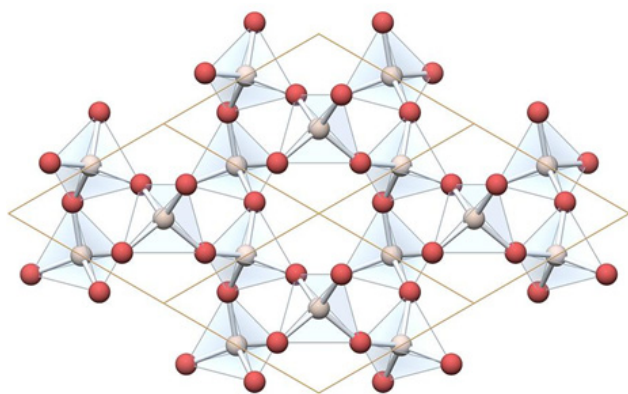
Figure 7. A 2×2 diagram of the repeating structure of quartz (SiO$_2$). (Reproduced with a permission from [27]. Copyright 2013.)
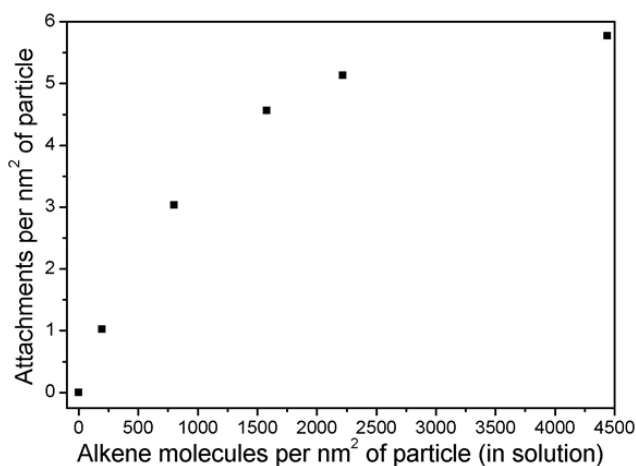

Figure 8. Controlling thiol–ene functionalization through 11-bromo-1-undecene added to system (reaction time: 60 min).

Figure 9. Tracking 11-bromo-1-undecene molecular ion (223 *m/z*) peak area as a function of concentration pre- and post-functionalization.

the ATR-FTIR analysis method above, and verifies the result provided by the FTIR analysis technique.

To verify the accessibility of sites for covalent attachment, absolute cell lengths that are generally used for quartz at 1 atm are 0.491 33 and 0.540 53 nm [26] were considered, and show a helical structure. A graphical adaptation [27] of these lattice constants is shown in figure 7, in a 2×2 cell structure in the *x*–*y* plane [26], in which oxygen atoms are represented by red spheres at the verticies of the tetrahedrons and the silicon atoms are at the centre. This structure results in an average of 11.3 surface (or near surface) silicon atoms per nm^2.

It should be noted that quartz contains a silicon atom with four oxygen atoms attached, however, in our case, only three oxygen atoms are attached to each silicon atom with the remaining bond corresponding to a mecraptopropyl group in which the sulphur atom is approximately 0.4 nm from the silicon atom, providing access from near surface silicon atoms. For charge stability reasons, it can be expected that the thiol groups will be oriented out of the surface, and that silicon atoms a couple of layers deep would be able to present reactive thiol units to the surface of the particle.

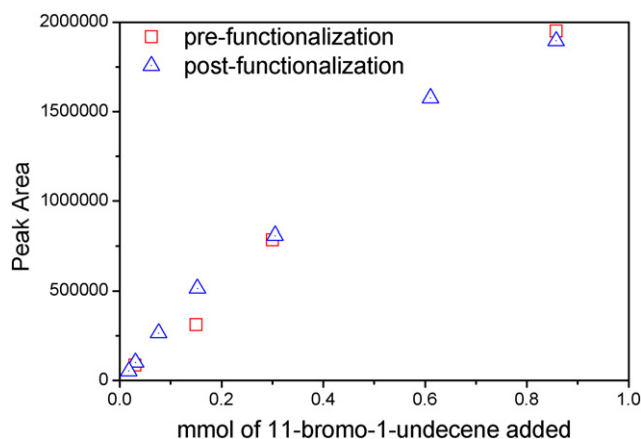Taking an irradiation time of 60 min as the limiting attachment condition, figure 8 shows the impact of the

concentration of alkene 11-bromo-1-undecene in solution on the attachment density. Surprisingly, despite the very large excess of alkene over stoichiometric addition—of the order of 10^2 and 10^3 molar—as the excess of alkene is decreased, the surface attachment also decreases.

Figure 9 shows that during the washing procedure of the particles, the excess of alkene required for functionalization can be accounted for in solution. The similar peak area of the molecular ion of 11-bromo-1-undecene ($m/z = 223$) pre- and post-functionalization indicates the concentration of alkene does not change significantly during reaction over a wide range of initial concentrations and importantly, homopolymerization of the alkene does not occur. Further addition of the radical generating photoinitiator does not result in any further increase in the surface attachment density, supporting the conclusion that attachment density is limited by access to surface functionality.

The apparent limitation of attachment density based on alkene concentration in solution and the dependence on UV irradiation time provides the opportunity to control the number of attachments. Further, it provides an opportunity to attach more than one moiety through sequential reactions in predetermined and controlled amounts creating multifunctional particles. This sequential attachment of multiple alkenes has been demonstrated by first photo irradiating 0.27 mmol of 11-bromo-1-undecene (corresponding to 570 molecules per nm^2 in solution) for 35 min resulting in 1.6 attachments per nm^2. Particles are then washed and 1-octadecene is introduced at the same concentration and fresh benzophenone resulting in a total of 2.2 attachments per nm^2, an increase in decoration density of 0.6 attachments per nm^2.

4. Conclusion

A simple method to quantify the functionalization density of SiNPs is demonstrated using ATR-FTIR. The technique is applicable to a broad range of IR active functional groups, provided isolated resonances can be found. In this case, tracking the sp^2 hydrocarbon absorbance ν_{asym} (CH$_2$)

at $2926\,\mathrm{cm}^{-1}$ is a convenient absorbance in conjunction with the ν_{sym} (Si–O–Si) bending peak at $1070\,\mathrm{cm}^{-1}$ as the reference band. The Si–O–Si band is typically well separated from the types of bands normally utilized, providing a convenient reference. The high throughput, non-destructive technique that is available in most laboratories provides a reliable method for the characterization of functionalized nanoparticles.

Attachment densities of about 5 adducts per nm^2 have been achieved with thiol–ene click chemistry, which is significantly higher than previously reported. Importantly, an excess of alkene of the order of 10^2–10^3 is required to achieve these densities, which may have been a limitation in previous cases. The attachment density showed a strong nonlinear dependence on the concentration of alkene in solution and with irradiation time indicating that accessability of reactive sites is the limiting factor, although attachment densities of greater than 4.9 adducts per nm^2 could not be obtained. TGA results confirmed the attachment density.

The ability to create multifunctional SiNPs was demonstrated through a sequential reaction. By limiting the attachment density of a first alkene, isolating the SiNPs, and redispersing in the presence of a second alkene an increase in attachment density from 1.6 to 2.2 attachments per nm^2 was obtained.

The potential for the production of high attachment density SiNPs with tunable, multiple surface functionalities provides a platform for a range of applications including surface specific sensors and medical imaging.

Acknowledgments

References

[1] Ambrogio M W *et al* 2011 Mechanized silica nanoparticles: a new frontier in theranostic nanomedicine *Account. Chem. Res.* **44** 903–13

[2] Awaad A, Nakamura M and Ishimura K 2012 Histochemical and biochemical analysis of size-dependant nanoimmunoresponse in mouse Peyer's patches using fluorescent organosilica particles *Int. J. Nanomed.* **7** 1423–39

[3] Kumar R *et al* 2006 Template removal and thermal stability of organically functionalized mesoporous silica nanoparticles *Chem. Mater.* **18** 4319–27

[4] Klabunde K J 2001 *Nanoscale Materials in Chemistry* (New York: Wiley-Interscience)

[5] Schubert U H 2004 *Synthesis of Inorganic Materials* (Weinheim: Wiley-VCH)

[6] Wei G-T *et al* 2004 Aqueous-organic phase transfer of gold nanoparticles and gold nanorods using an ionic liquid *J. Am. Chem. Soc.* **126** 5036–7

[7] Goulet P J G, Bourret G R and Lennox R B 2012 Facile phase transfer of large, water-soluble metal nanoparticles to nonpolar solvents *Langmuir* **28** 2909–13

[8] McMahon J M and Emory S R 2006 Phase transfer of large gold nanoparticles to organic solvents with increased stability *Langmuir* **23** 1414–8

[9] Sekiguchi S *et al* 2012 Hydrophilic gold nanoparticles adaptable for hydrophobic solvents *Langmuir* **28** 5503–7

[10] Saunders B R and Vincent B 1999 Microgel particles as model colloids: theory, properties and applications *Adv. Colloid Interface Sci.* **80** 1–25

[11] Nakamura M and Ishimura K 2008 One-pot synthesis and characterization of three kinds of thiol–organosilica nanoparticles *Langmuir* **24** 5099–108

[12] Nickless G 1968 *Inorganic Sulfur Chemistry* (Amsterdam: Elsevier)

[13] Killops K L, Campos L M and Hawker C J 2008 Robust, efficient, and orthogonal synthesis of dendrimers via thiol–ene 'click'chemistry *J. Am. Chem. Soc.* **130** 5062–4

[14] Hoyle C E, Lowe A B and Bowman C N 2010 Thiol-click chemistry: a multifaceted toolbox for small molecule and polymer synthesis *Chem. Soc. Rev.* **39** 1355–87

[15] Rutledge R D *et al* 2010 Thiol–ene induced diphosphonic acid functionalization of superparamagnetic iron oxide nanoparticles *Langmuir* **26** 12285–92

[16] Ethirajan A *et al* 2013 UV-induced functionalization of poly(divinylbenzene) nanoparticles via efficient [2+2]-photocycloadditions. *Polym. Chem.* **4** 4010–6

[17] Joso R *et al* 2009 Facile access to hydroxy-functional core–shell microspheres via grafting of ethylene oxide by anionic ring-opening polymerization *Macromol. Rapid Commun.* **30** 1009–14

[18] Nakamura M *et al* 2011 One-pot synthesis and characterization of dual fluorescent thiol-organosilica nanoparticles as non-photoblinking quantum dots and their applications for biological imaging *J. Mater. Chem.* **21** 4689–95

[19] Li Y X A Q 2007 Multiple fluorescent labeling of silica nanoparticles with lanthanide chelates for highly sensitive time-resolved immunofluorometric assays *Clin. Chem.* **53** 1503–10

[20] Dabrowski J A M, H-J 2000 Silicon surfaces and formation of interfaces *Basic Science in the Industrial World* (Singapore: World Scientific)

[21] Skoog D A, Holler J F and Crouch S R 2007 *Principles of Instrumental Analysis* 6th edn (Belmont: Thomson Brooks/Cole)

[22] Duyckaerts G 1959 The infra-red analysis of solid substances—a review *Analyst* **84** 201–14

[23] Štaudner E *et al* 1992 Infrared spectrophotometry of maleic anhydride terpolymers *Eur. Polym. J.* **28** 1147–50

[24] Bellamy M K 2010 Using FTIR-ATR spectroscopy to teach the internal standard method *J. Chem. Educ.* **87** 1399–401

[25] Khire V S, Lee T Y and Bowman C N 2008 Synthesis, characterization and cleavage of surface-bound linear polymers formed using thiol–ene photopolymerizations *Macromolecules* **41** 7440–7

[26] Levien L, C T P and Weidner D J 1980 Structure and elastic properties of quartz at pressure *Am. Mineral.* **65** 920–30

[27] Akhavan A C 2013 *The Quartz Page* Available from www.quartzpage.de